

What is the coordination number of vanadium in vanadyl nitrate, VO(NO₃)₃? A study of its molecular structure in the gas phase by electron diffraction and *ab initio* calculations

Bruce A. Smart,^a Heather E. Robertson,^a David W. H. Rankin,^{*a} Eric G. Hope^b and Colin J. Marsden^c

^a Department of Chemistry, University of Edinburgh, West Mains Rd., Edinburgh, UK EH9 3JJ. E-mail: d.w.h.rankin@ed.ac.uk

^b Department of Chemistry, University of Leicester, Leicester, UK LE1 7RH

^c Laboratoire de Physique Quantique, IRSAMC, CNRS-UMR 5626, Université P. Sabatier, 118 route de Narbonne, 31062 Toulouse Cedex 04, France

Received 27th August 1998, Accepted 2nd December 1998

The structure of isolated vanadyl nitrate, VO(NO₃)₃, has been determined in the gas phase by electron diffraction (GED) and molecular orbital calculations. VO(NO₃)₃ adopts a structure which is best described as being based on a distorted pentagonal bipyramid with overall C_s symmetry. The structure contains three bidentate planar nitrate groups bound asymmetrically to the vanadium atom. A single nitrate group lies in the mirror plane, while the two others are on either side of that plane and almost perpendicular to it. Important structural parameters are: V(1)=O(2) 160.7(7), V(1)–O(3) 191.5(7), V(1)⋯O(6) 225.8(20), V(1)–O(7) 197.1(5), V(1)⋯O(9) 215.4(9) pm, O(2)–V(1)–O(3) 94.5(13), O(2)–V(1)–O(7) 96.3(9), O(2)–V(1)–O(6) 155.8(13), V(1)–O(3)–N(4) 99.5(8), V(1)–O(7)–N(8) 96.9(4) and N(8)–V(1)–O(2)–N(4) 113.2(3)°.

Introduction

The nitrate group as a ligand has been extensively investigated, since it displays an unusually versatile coordination chemistry. No fewer than nine different coordination modes have been identified and analysed in a review article.¹ In general, the nitrate ligand is bidentate and its particularly small bite of less than 220 pm allows metals to display unusually high coordination numbers. Thus both Ti(NO₃)₄ and [Co(NO₃)₄][−] contain 8-coordinate metal ions,² though the coordination is symmetric about Ti but asymmetric about Co. Bridging bidentate nitrate ligands are found in Cu(NO₃)₂.³ In [Sc(NO₃)₅]^{2−} the Sc is 9-coordinate, as one of the nitrate groups is monodentate, whereas in the valence-isoelectronic species [Y(NO₃)₅]^{2−} all the nitrate groups are bidentate.⁴ Only monodentate nitrate ligands are found in [Au(NO₃)₄][−].⁵ These examples show that it is not generally possible to deduce the type of coordination in a nitrate complex just from its stoichiometry.

The oxo-nitrato species vanadyl nitrate, VO(NO₃)₃, has been known for over 40 years,⁶ yet its structure is not known with any certainty. An unpublished electron diffraction study, describing work on the low-energy photoelectron spectra of gas-phase nitrate complexes,⁷ indicated a bidentate coordination of the nitrate ligands giving a pentagonal-bipyramidal arrangement of oxygen atoms around the vanadium atom. A similar conclusion was reached from studies of the vibrational spectra in both gaseous and liquid phases,^{8,9} although not all the spectral features can readily be rationalised in terms of the C_s model favoured by the authors. It is not immediately clear whether the very small V(v) ion can support a coordination number as high as seven if all the ligands are strongly bound. Only for the crystallographically characterised adduct VO(NO₃)₃·CH₃CN is the ligand arrangement established beyond doubt.¹⁰ This species has an essentially pentagonal-bipyramidal structure in which the five oxygen atoms that make up the pentagonal plane originate from one monodentate and two effectively symmetric bidentate nitrate ligands. The authors surmise that the aceto-

nitrile ligand has displaced the oxygen atom *trans* to the vanadyl oxygen and that this oxygen is presumably relatively weakly bound to vanadium in vanadyl nitrate.

The gas-phase structure of chromyl nitrate, CrO₂(NO₃)₂, was studied a few years ago,¹¹ revealing an intriguing coordination geometry containing asymmetric bidentate groups with Cr–O distances differing by as much as 30 pm. To pursue further the preferred binding modes of the nitrate group we decided to study vanadyl nitrate in detail. Here we report its molecular structure as obtained from a combined electron diffraction and computational study using the SARACEN method.¹²

Experimental

Synthesis

Vanadyl nitrate was prepared by the literature method,¹³ and the purity established using liquid phase IR spectroscopy.^{8,9} IR spectra were recorded on a Digilab FTS40 FTIR spectrometer operating at 2 cm^{−1} resolution for a liquid sample compressed between KBr discs under an inert atmosphere.

Ab initio calculations

As vanadyl nitrate is a complicated molecule by the standards of gas-phase electron diffraction, it was clear from the outset that its structure could not be obtained with any reliability without considerable support from computational methods. The SARACEN technique¹² allows one to use data from various sources, weighted according to their presumed reliability, in a global least-squares refinement procedure. Transition-metal compounds are rather more difficult to treat by theoretical techniques than “standard” organic or main-group systems, so we felt it important to try to establish which computational method would give the most reliable results and to calibrate their quality. As a minimum requirement, a good description of the structure of isolated nitric acid is clearly essential. We compare in Table 1 the (equilibrium or *r_e*) experimental values¹⁴

Table 1 Comparison of optimised and experimental structural parameters for nitric acid^a

Parameter	SCF	MP2	BLYP	B3LYP	Expt.
N–O(H)	133.9	142.1	148.2	141.8	141.0
N=O _c	118.8	122.5	123.0	121.5	121.3
N=O _t	117.1	121.4	121.3	119.9	119.8
O–N=O _c	115.9	115.4	115.2	115.5	115.7
O–N=O _t	114.9	113.7	113.4	114.0	114.1

^a Distances in pm and angles in degrees. TZP basis used; see text. Experimental values from ref. 10.

and the results obtained using four standard theoretical methods with a flexible basis set of triple-zeta-plus-polarisation (TZP) quality. The Huzinaga–Dunning (10,6)/[5,3] bases for N and O were employed, together with the 5/3 set for hydrogen.¹⁵ Polarisation exponents of 0.8 for N, 0.9 for O and 0.75 for H were adopted, together with the pure spherical-harmonic representation of the d-type functions. The Gaussian series of programs were used in all computations.¹⁶

It is clear from Table 1 that the SCF method gives bond distances which are too short, particularly where electronegative atoms are involved, as is already well known.¹⁷ For a molecule of the complexity of vanadyl nitrate, with as many as 21 independent geometrical parameters under C_s symmetry, it is also clear that treatments of electron correlation must be inexpensive, with efficient implementations of gradient methods. The geometry predicted by the MP2 method is certainly far superior to that obtained at the SCF level. Density functional theory (DFT) is now very popular, as its cost effectiveness is usually high and its computational demands scale less unfavourably with increasing molecular size than those of traditional *ab initio* methods. In the case of nitric acid, the so-called BLYP variety of DFT is only slightly more successful than the SCF method, as it leads to bonds which are appreciably too long, particularly for the N–O single bond. However, the hybrid version of DFT known as B3LYP performs rather well for nitric acid, and in fact is a little more successful for this case than is MP2 theory.

As a further, presumably more demanding, test of the quality of the MP2 and B3LYP methods for structure prediction, we decided to check their reliability for CrO_2F_2 . This molecule, whose structure is well established,¹⁸ contains both M=O double bonds comparable to that in vanadyl nitrate and metal–ligand single bonds. It therefore seemed a suitable calibration vehicle. It is already known that the SCF method gives a particularly poor account of the Cr=O bonds in that case.¹¹ Although the use of density functional methods has already been recommended for molecules such as CrO_2F_2 ,¹⁹ we felt it worthwhile to quantify the accuracy attainable for the structural parameters with a large basis set. An all-electron basis of triple-zeta quality in the valence region (14,9 + 2,6)/(9,5 + 2,4)²⁰ was adopted for Cr, augmented by a set of f-type polarisation functions, whose exponent was roughly optimised at the B3LYP level to 0.7 in CrO_2F_2 (it has been shown that use of a large-core pseudopotential is dangerous for chromium in high oxidation states).¹¹ The oxygen basis was that already described above, and an analogous basis was adopted for F; d-type polarisation exponents were optimised for both O (0.85) and F (0.9) in CrO_2F_2 .

The geometry predicted for CrO_2F_2 using the B3LYP method and the TZP basis described above (the variationally optimum B3LYP f-type exponent for Cr was found to be 0.7) was rather successful. Optimised (experimental) geometrical parameters are $r(\text{Cr}=\text{O})$ 155.3 (157.2), $r(\text{Cr}-\text{F})$ 171.4 (171.6) pm, $\text{O}=\text{C}=\text{O}$ 108.4 (107.8) and $\text{F}-\text{Cr}-\text{F}$ 109.8 (111.9)°. Much less success was obtained with the MP2 method, which gave absurdly non-physical force constants that were remarkably sensitive to geometry. The optimisation procedure proved to be numerically

unstable, and the stationary point was located only with considerable difficulty. As the optimised parameters are 166.5 and 178.5 pm, 103.1 and 114.9° for $r(\text{Cr}=\text{O})$, $r(\text{Cr}-\text{F})$, $\text{O}=\text{C}=\text{O}$ and $\text{F}-\text{Cr}-\text{F}$, respectively, it is clear that the MP2 structure is not close to experiment.

In an attempt to uncover the reason(s) for the unsatisfactory geometrical predictions yielded by the MP2 method for CrO_2F_2 , we performed a CISD calculation, which indicated that the Hartree–Fock reference configuration makes up about 91% of the CISD wavefunction. The largest coefficient for an excited configuration was found to be 0.039. It therefore appears that the multi-reference character of CrO_2F_2 is not negligible, even if no single excited configuration dominates. In these circumstances, convergence of the MP perturbation series is unpredictable. It was beyond the scope of this work to explore this point in detail; we decided that MP2 theory could not be expected to perform well for molecules such as vanadyl nitrate, which are closely related to CrO_2F_2 , and therefore used the B3LYP method for our final structural predictions. An exponent of 0.6 was adopted for the f-type functions on vanadium.

Electron diffraction

Electron scattering intensities were recorded on Kodak Electron Image plates using the Edinburgh gas diffraction apparatus operating at *ca.* 44.5 kV (electron wavelength *ca.* 5.6 pm).²¹ Nozzle-to-plate distances for the metal inlet nozzle were *ca.* 95 and 259 mm yielding data in the s range 20–224 nm^{-1} ; 3 plates were exposed at each camera distance. The sample and nozzle temperatures were maintained at 360 K during the exposure periods.

The scattering patterns of benzene were also recorded for the purpose of calibration; these were analysed in exactly the same way as those for vanadyl nitrate so as to minimise systematic errors in the wavelengths and camera distances. Nozzle-to-plate distances, weighting functions used to set up the off-diagonal weight matrix, correlation parameters, final scale factors and electron wavelengths for the measurements are collected in Table 2.

The electron-scattering patterns were converted into digital form using a computer-controlled Joyce Loebel MDM6 microdensitometer with a scanning program described elsewhere.²² The programs used for data reduction²² and least-squares refinement²³ have been described previously; the complex scattering factors were those listed by Ross *et al.*²⁴

Results

Theoretical computations

Since even the gross features of the coordination geometry about the vanadium atom in vanadyl nitrate were not clearly established before this work, and since the ED method alone could not possibly exclude the presence of several isomers or conformers, the initial computational task was to explore the conformational space in some detail. This initial phase of the study was performed at the SCF level with a DZP basis, which was shown to be quite reliable for this purpose for chromyl nitrate.¹¹ After extensive searching, three stationary points were found. The first of these had C_s symmetry, and corresponded to the structure reported in this article; it was shown to be a true minimum. One $\text{O}=\text{V}-\text{O}-\text{N}$ dihedral angle is 180° and two are close to ±90°; the unique nitrate group is appreciably asymmetric, with V–O distances which differ by about 30 pm, but the two symmetry-related nitrates are coordinated more symmetrically, with calculated V–O distances differing by less than 10 pm.

The second stationary point also has C_s symmetry; in this case, the unique $\text{O}=\text{V}-\text{O}-\text{N}$ dihedral angle is zero while the other two are close to ±83°. In this structure the unique nitrate

Table 2 Nozzle-to-plate distances (mm), weighting functions (nm^{-1}), correlation parameters, scale factors and electron wavelengths (pm) used in the electron diffraction study

Nozzle-to-plate distance ^a	Δs	s_{min}	s_{w1}	s_{w2}	s_{max}	Correlation parameter	Scale factor ^b	Electron wavelength
94.75	4	80	100	200	224	-0.396	0.614(14)	5.683
258.57	2	20	40	140	164	0.487	0.874(10)	5.680

^a Determined by reference to the scattering pattern of benzene vapour. ^b Values in parentheses are the estimated standard deviations.

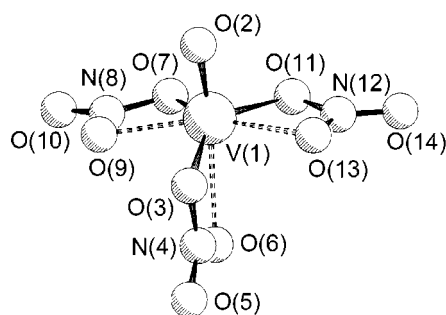


Fig. 1 Molecular structure of $\text{VO}(\text{NO}_3)_3$.

group is clearly monodentate, as the unique V–O distance is only 181 pm but the two others are both over 300 pm. The unique V–O–N bond angle is large (138°), presumably to alleviate steric repulsions involving the vanadyl oxygen atom. This conformer is 61 kJ mol^{-1} less stable than the first at the TZP/SCF level, with the gap reducing to 48 kJ mol^{-1} in the TZP/B3LYP calculation; more importantly, it is a transition state, with an imaginary a'' vibrational motion which involves a concerted torsional motion of the nitrate groups, leading towards the minimum previously described. The final stationary point had C_{3v} symmetry (optimisations under C_3 symmetry converged towards C_{3v}). The O=V–O–N dihedral angles are all zero, as the alternative of 180° would lead to intolerable inter-nitrate steric distress, unless the V–O–N angle became exceedingly large. That angle is 135° in the optimised geometry, leading to $\text{O}\cdots\text{O}$ distances involving the vanadyl oxygen of 270 pm, close to the sum of the van der Waals radii. This C_{3v} structure lies 115 (TZP/SCF) or 76 (TZP/B3LYP) kJ mol^{-1} above the global minimum and has two (degenerate) imaginary vibrational frequencies involving torsions of the nitrate groups. The energies of the second and third stationary states are thus far too high to be of structural significance, and neither is a potential minimum.

Electron diffraction analysis

Since only one true minimum was located in the theoretical computations described above, the electron diffraction refinements were carried out on a single species, shown in Fig. 1. C_s symmetry was adopted and the VONO_2 groups were assumed to be planar, as insignificant deviations from planarity (torsion angles differing from 0 or 180° by no more than 0.5°) were found in the various computations. The structure of vanadyl nitrate was defined in terms of 19 independent geometric parameters including 9 bond length, 8 bond angle and 2 torsion parameters. Bond length parameters are V(1)=O(2), p_1 , the mean and difference of V(1)–O(3) and V(1)–O(7) bond lengths, p_2 and p_3 , the average N–O bond, p_4 , the difference between the weighted averages of the N–O bond lengths of the VO_2N four membered rings and the terminal (double) N–O bonds, p_5 , the differences between N(8)–O(7) and N(8)–O(9), N(4)–O(3), or N(4)–O(6) bonds, p_6 – p_8 and the difference between N(8)–O(10) and N(4)–O(5) bonds, p_9 . Bond angle parameters include the mean and difference of O(2)–V(1)–N(8) and O(2)–V(1)–N(4) angles, p_{10} and p_{11} , the mean and difference of V(1)–O(7)–N(8) and V(1)–O(3)–N(4) angles, p_{12} and p_{13} , the average of O(3)–N(4)–O(5), O(3)–N(4)–O(6), O(7)–N(8)–O(9) and O(7)–N(8)–

Table 3 Refined and calculated geometric parameters for $\text{VO}(\text{NO}_3)_3$ (distances in pm, angles in degrees) from the GED study^{a,b}

No.	Parameter	GED (r_a)	TZP/B3LYP (r_e)
p_1	V(1)–O(2)	160.7(7)	155.4
p_2	[V(1)–O(3) + V(1)–O(7)]/2	194.3(4)	200.1
p_3	V(1)–O(3) – V(1)–O(7)	-5.7(10)	-5.4
p_4	N–O _{av}	124.0(2)	126.2
p_5	N–O _{rav} – N–O _{tav}	11.6(9)	10.7
p_6	N(8)–O(7) – N(8)–O(9)	1.3(5)	1.3
p_7	N(8)–O(7) – N(4)–O(3)	-2.7(5)	-2.8
p_8	N(8)–O(7) – N(4)–O(6)	3.3(5)	3.4
p_9	N(8)–O(10) – N(4)–O(5)	-0.6(5)	-0.6
p_{10}	[O(2)–V(1)–N(8) + O(2)–V(1)–N(4)]/2	111.0(6)	116.1
p_{11}	O(2)–V(1)–N(8) – O(2)–V(1)–N(4)	-29.7(17)	-30.3
p_{12}	[V(1)–O(7)–N(8) + V(1)–O(3)–N(4)]/2	98.2(5)	96.9
p_{13}	V(1)–O(7)–N(8) – V(1)–O(3)–N(4)	-2.6(8)	-3.7
p_{14}	O–N–O _{av}	119.0(6)	116.9
p_{15}	O–N–O _{avd}	0.9(5)	0.5
p_{16}	[O(7)–N(8)–O(9) – O(7)–N(8)–O(10)]	-13.9(9)	-14.8
p_{17}	[O(3)–N(4)–O(5) – O(3)–N(4)–O(6)]	9.5(10)	8.9
p_{18}	NO_3 twist	2.0(14)	0.4
p_{19}	N(4)–V(1)–O(2)–N(8)	113.2(3)	110.0
Dependent parameters			
p_{20}	V(1)–O(3)	191.5(7)	197.3
p_{21}	V(1)–O(6)	225.8(20)	225.0
p_{22}	V(1)–O(7)	197.1(5)	202.8
p_{23}	V(1)–O(9)	215.4(9)	208.0
p_{24}	N(4)–O(3)	131.0(6)	133.2
p_{25}	N(4)–O(5)	116.7(8)	119.4
p_{26}	N(4)–O(6)	125.1(5)	127.0
p_{27}	N(8)–O(7)	128.3(4)	130.3
p_{28}	N(8)–O(9)	127.1(4)	129.0
p_{29}	N(8)–O(10)	116.1(7)	118.8
p_{30}	O(2)–V(1)–O(3)	94.5(13)	100.1
p_{31}	O(2)–V(1)–O(7)	96.3(9)	103.0
p_{32}	V(1)–O(3)–N(4)	99.5(8)	98.8
p_{33}	V(1)–O(7)–N(8)	96.9(4)	95.0
p_{34}	O(3)–N(4)–O(5)	123.3(3)	121.2
p_{35}	O(3)–N(4)–O(6)	113.8(8)	112.2
p_{36}	O(5)–N(4)–O(6)	122.8(14)	126.6
p_{37}	O(7)–N(8)–O(9)	112.5(5)	109.8
p_{38}	O(7)–N(8)–O(10)	126.5(9)	124.6
p_{39}	O(9)–N(8)–O(10)	121.0(13)	125.6

^a Figures in parentheses are the estimated standard deviations of the last digits. ^b See text for parameter definitions.

O(10) angles, p_{14} , the difference between the average of the O(7)–N(8)–O(9) and O(7)–N(8)–O(10) angles and the average of the O(3)–N(4)–O(5) and O(3)–N(4)–O(6) angles, p_{15} , the difference between O(7)–N(8)–O(9) and O(7)–N(8)–O(10), p_{16} , and the difference between O(3)–N(4)–O(5) and O(3)–N(4)–O(6), p_{17} . The torsion angles are a clockwise twist of equivalent nitrate groups away from a structure in which the plane of the nitrate group is perpendicular to the O(2)–V(1)–N(8) plane, p_{18} , and the N(4)–V(1)–O(2)–N(8) dihedral angle, p_{19} . The atom numbering is shown in Fig. 1 and a list of the independent geometric parameters is given in Table 3.

The starting parameters for the r_a refinement were taken from the theoretical geometries optimised at the TZP/B3LYP level. Theoretical (DZP/BLYP) Cartesian force fields were obtained and converted into force fields described by a set of symmetry coordinates using the ASYM40 program.²⁵ The presence of a

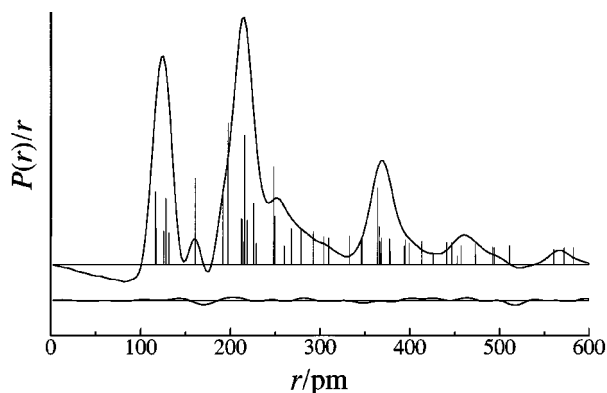


Fig. 2 Experimental and difference (experimental – theoretical) radial-distribution curves, $P(r)/r$, for $\text{VO}(\text{NO}_3)_3$. Before Fourier inversion the data were multiplied by $s \cdot \exp(-0.00002s^2)/(Z_N - f_N)$ ($Z_N - f_N$).

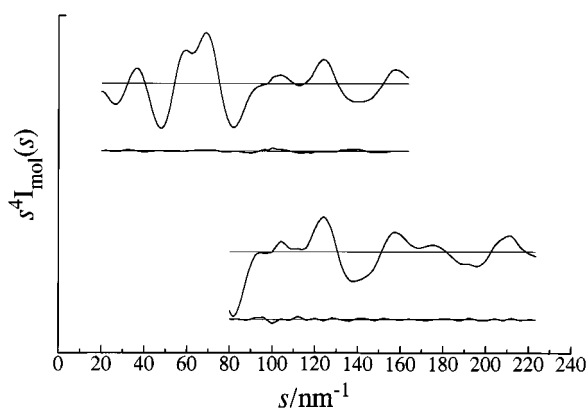


Fig. 3 Experimental and final weighted difference (experimental – theoretical) molecular-scattering intensities for $\text{VO}(\text{NO}_3)_3$.

number of low-frequency vibrational modes (64, 76, 97, 105, 142 and 147 cm^{-1} at the DZP/BLYP level) led to overestimated predictions of the perpendicular amplitudes of vibration (k). Since these values were considered unreliable, corrections for shrinkage effects were not included.

The use of the SARACEN method¹² (20 restraints) allowed the refinement of all 19 geometric parameters and 15 groups of vibrational amplitudes. The success of the final refinement, for which $R_G = 0.066$, can be assessed on the basis of the radial distribution curve (Fig. 2) and the molecular scattering intensity curves (Fig. 3). Final refined parameters are listed in Table 3, restraints used in the refinement in Table 4, interatomic distances and the corresponding amplitudes of vibration in Table 5 and the least-squares correlation matrix in Table 6.

Discussion

The structure of isolated vanadyl nitrate is best described as being based on a distorted pentagonal bipyramid with overall C_s symmetry (see Fig. 1). The coordination number of vanadium is thus seven, although three oxygen atoms are not fully bonded to vanadium. The structure contains bidentate nitrate groups bound asymmetrically to the vanadium atom. A single nitrate group lies in the mirror plane, while the two others are on either side of that plane and almost perpendicular to it. The degree of asymmetry in the nitrate coordination is far more pronounced for the unique nitrate group than for the two equivalent ones, as discussed in more detail below. Axial positions are occupied by the vanadyl oxygen atom [O(2)] and the more weakly bound oxygen [O(6)] of the nitrate group lying in the C_s plane, though the distortion of the bipyramid is sufficient to reduce the O(2)–V–O(6) angle from the idealised value of 180 to $155.8(13)^\circ$. The five equatorial positions are occupied by

Table 4 Restraints used in the refinement of the structure of $\text{VO}(\text{NO}_3)_3$ (distances in pm, angles in degrees) from the GED study^a

No.	Parameter	Refined value	Restraint
p_3	V(1)–O(3) – V(1)–O(7)	5.7(10)	–5.4(10)
p_5	N–O _{rav} – N–O _{tav}	11.6(9)	10.7(20)
p_6	N(8)–O(7) – N(8)–O(9)	1.3(5)	1.3(5)
p_7	N(8)–O(7) – N(4)–O(3)	–2.7(5)	–2.8(5)
p_8	N(8)–O(7) – N(4)–O(6)	3.3(5)	3.4(5)
p_9	N(8)–O(10) – N(4)–O(5)	–0.6(5)	–0.6(5)
p_{11}	O(2)–V(1)–N(8) – O(2)–V(1)–N(4)	–29.7(17)	–30.3(30)
p_{13}	V(1)–O(7)–N(8) – V(1)–O(3)–N(4)	–2.6(8)	–3.7(10)
p_{15}	O–N–O _{avd}	0.9(5)	0.5(5)
p_{16}	[O(7)–N(8)–O(9) – O(7)–N(8)–O(10)]	–13.9(9)	–14.8(10)
p_{17}	[O(3)–N(4)–O(5) – O(3)–N(4)–O(6)]	9.5(10)	8.9(10)
p_{18}	NO_3 twist	2.0(14)	0.4(20)
u_1	$u[\text{V}(1)–\text{O}(2)]$	3.9(4)	3.7(4)
u_{17}	$u[\text{O}(7) \cdots \text{O}(9)]$	4.6(5)	5.2(5)
u_{27}	$u[\text{O}(10) \cdots \text{O}(14)]$	12.8(12)	12.3(12)
u_{31}	$u[\text{O}(7) \cdots \text{O}(6)]$	23.1(18)	20.9(20)
u_{35}	$u[\text{N}(4) \cdots \text{O}(9)]$	15.6(11)	15.1(15)
u_{41}	$u[\text{O}(6) \cdots \text{O}(10)]$	21.6(24)	25.7(25)
u_{43}	$u[\text{O}(5) \cdots \text{O}(7)]$	19.9(16)	17.7(17)
u_{47}	$u[\text{O}(5) \cdots \text{O}(10)]$	30.1(20)	28.5(28)

^a Figures in parentheses are the estimated standard deviations of the last digits.

Table 5 Selected interatomic distances and mean amplitudes of vibration for $\text{VO}(\text{NO}_3)_3$ from the GED study^a

Atom pair	r_a/pm		u/pm
V(1)–O(2)	160.7(7)	u_1	3.9(4)
V(1)–O(3)	191.5(7)	u_2	8.8 (tied to u_4)
V(1)–O(6)	225.8(20)	u_3	8.4 (tied to u_4)
V(1)–O(7)	197.1(5)	u_4	9.3(8)
V(1)–O(9)	215.4(9)	u_5	10.3 (tied to u_4)
N(4)–O(3)	131.0(6)	u_6	5.0 (tied to u_{11})
N(4)–O(5)	116.7(8)	u_7	3.8 (tied to u_{11})
N(4)–O(6)	125.1(5)	u_8	4.4 (tied to u_{11})
N(8)–O(7)	128.3(3)	u_9	4.6 (tied to u_{11})
N(8)–O(9)	127.1(4)	u_{10}	4.5 (tied to u_{11})
N(8)–O(10)	116.1(7)	u_{11}	3.8(7)
V(1) \cdots N(4)	249.2(14)	u_{12}	10.8 (tied to u_{13})
V(1) \cdots N(8)	247.7(7)	u_{13}	9.8(7)
O(3) \cdots O(5)	218.2(11)	u_{14}	5.0 (tied to u_{17})
O(3) \cdots O(6)	214.6(11)	u_{15}	4.8 (tied to u_{17})
O(5) \cdots O(6)	212.3(16)	u_{16}	4.6 (tied to u_{17})
O(7) \cdots O(9)	212.4(8)	u_{17}	4.6(5)
O(7) \cdots O(10)	218.3(10)	u_{18}	4.8 (tied to u_{17})
O(9) \cdots O(10)	211.6(14)	u_{19}	4.8 (tied to u_{17})
V(1) \cdots O(5)	365.2(13)	u_{20}	12.4 (tied to u_{21})
V(1) \cdots O(10)	363.8(7)	u_{21}	11.6(9)
O(3) \cdots O(9)	267.6(57)	u_{22}	15.4(15)
O(2) \cdots O(9)	278.1(23)	u_{23}	15.9 (tied to u_{22})
O(6) \cdots O(9)	292.4(36)	u_{24}	21.3 (tied to u_{22})
O(2) \cdots O(7)	267.6(20)	u_{25}	15.8 (tied to u_{22})
O(2) \cdots O(3)	259.5(27)	u_{26}	16.4 (tied to u_{22})
O(10) \cdots O(14)	662.5(112)	u_{27}	12.8(12)

^a See Fig. 1 for atom numbering; all other distances were included in the refinement, but are not listed here.

Table 6 Least-squares correlation matrix ($\times 100$) for $\text{VO}(\text{NO}_3)_3$ ^a

	p_2	p_5	p_{10}	p_{12}	p_{14}	u_4	u_{11}	u_{13}
p_1		–72				–67	72	
p_{11}			–64					
p_{12}				–63				
p_{13}				–56				
p_{19}					54			
u_{13}								
u_{21}	–50							83
u_{22}					–66			

^a Only elements with absolute values $>50\%$ are shown.

the more strongly bound oxygen atom of the unique nitrate group, O(3), and two oxygens atoms from each of the two symmetry-related nitrate groups. All nitrate groups and VO₂N rings are planar or essentially so.

These comments show that the authors of the X-ray study of the acetonitrile adduct of vanadyl nitrate¹⁰ were correct in supposing that the CH₃CN ligand had displaced an oxygen *trans* to the vanadyl oxygen in the free molecule. Many of the fine structural details discussed in that work are confirmed here, and established with greater precision. For example, we note that the longest V–O distance, V···O(6), is the one *trans* to the vanadyl oxygen; this bond is 34.3(21) pm longer than its partner in the unique nitrate group, whereas the difference in V–O bond lengths for the two symmetry-related nitrates is only half that, at 18.3(10) pm. The asymmetry within the nitrate groups is systematic, even if some of the differences may be of rather marginal statistical significance; the shorter V–O distance within the equivalent groups, V–O(7), occurs with the longer N–O bonds, while the shortest of all the N–O distances is that associated with the longest V–O bond and *vice versa*.

Overall, the agreement between the structures obtained by theory (TZP/B3LYP) and experiment is quite satisfactory, considering the complexity of the problem, with the largest differences being found for the various V–O interactions. The refined V=O distance of 160.7(7) pm is a little longer than might have been expected, but not worryingly so; since the experimental Cr=O distance in CrO₂F₂ exceeds the TZP/B3LYP value by 1.9 pm, as described above, the computed length of 155.4 pm for the V=O distance in vanadyl nitrate implies an experimental result of about 157.3 pm, with an uncertainty of perhaps 2 pm. The calculated difference between the two V–O bonds within the equivalent nitrate groups is large compared to the GED value, though the uncertainties in “difference” parameters of this type are always appreciable. It remains to be seen whether more elaborate theoretical treatments would have given better agreement with experiment. Presumably the systematic error in computed N–O distances, which are too long by some 2 pm, could be reduced. We note with satisfaction (see Table 4) that the refined results for the various restrained parameters do not differ significantly from the assumed input values; this shows that the ED data are quite compatible with the restraints adopted from the computation, and since the refined uncertainties are often smaller than those input, it is clear that the experimental data do contain information about these parameters.

Predicted bond angles are mostly within 2–3° of the experimental values, though the O(9)–N(8)–O(10) angle is a notable exception, as the difference of 7.2° amounts to more than seven nominal standard deviations. We suspect that the calculated values for bond angles are rather reliable for equilibrium values, and that some of the apparent differences, such as that noted above, may be a consequence of significant vibrational motion at the slightly elevated temperature of the GED experiment; it is quite impractical to use a dynamic model of large-amplitude molecular motion for a molecule as complex as vanadyl nitrate. It is noteworthy that there are some minor discrepancies in the assignment of the vibrational spectrum proposed in ref. 5, bands at 962.5 and 1612 cm⁻¹ in the Raman spectrum being depolarised rather than polarised. The authors of ref. 5 proposed that large-amplitude motion concerning O(6), *trans* to the vanadyl oxygen, might effectively lower the local symmetry. Furthermore, there is evidence for significant internal motion for related compounds, such as vanadyl carboxylate complexes, VO(OCOR)₃, from VT ¹H NMR spectroscopy, where two signals are observed at low temperature whereas only one signal is observed at room temperature as a result of a fluxional process.²⁶ It also seems possible that intermolecular interactions in condensed phases might perturb the spectrum.

Acknowledgements

We thank the EPSRC for financial support of the Edinburgh Electron Diffraction Service (grant GR/K44411), for the provision of microdensitometer facilities at the Daresbury Laboratory and for the Edinburgh *ab initio* facilities (grant GR/K04194). We thank the Royal Society for financial support (E. G. H.) and the IDRIS for their support for theoretical work in Toulouse (projects 940444 and 981104).

References

- 1 C. C. Addison, N. Logan, S. C. Wallmark and C. D. Garner, *Quart. Rev.*, 1971, **25**, 289.
- 2 J. G. Bergman and F. A. Cotton, *Inorg. Chem.*, 1966, **5**, 1208.
- 3 C. C. Addison and A. Walker, *Proc. Chem. Soc.*, 1961, 242.
- 4 C. C. Addison, A. J. Greenwood, M. J. Haley and N. Logan, *J. Chem. Soc., Chem Commun.*, 1978, 580.
- 5 C. D. Garner and S. C. Wallwork, *Chem. Commun.*, 1969, 108.
- 6 M. Schmeisser, *Angew. Chem.*, 1955, **67**, 493.
- 7 C. D. Garner, R. W. Hawksworth, I. H. Hillier, A. A. MacDowell and M. F. Guest, *J. Am. Chem. Soc.*, 1980, **102**, 4325.
- 8 C. D. Addison, D. W. Amos, D. Sutton and W. H. H. Hoyle, *J. Chem. Soc. A*, 1967, 808.
- 9 S. A. Brandan, A. B. Altabef and E. L. Varetti, *Spectrochim. Acta, Part A*, 1995, **51**, 669.
- 10 F. W. B. Einstein, E. Enwall, D. M. Morris and D. Sutton, *Inorg. Chem.*, 1971, **10**, 678.
- 11 C. J. Marsden, K. Hedberg, M. M. Ludwig and G. L. Gard, *Inorg. Chem.*, 1991, **30**, 4761.
- 12 A. J. Blake, P. T. Brain, H. McNab, J. Miller, C. A. Morrison, S. Parsons, D. W. H. Rankin, H. E. Robertson and B. A. Smart, *J. Phys. Chem.*, 1996, **100**, 12280.
- 13 A. D. Harris, J. C. Trebellas and H. B. Jonassen, *Inorg. Synth.*, 1967, **9**, 83.
- 14 A. P. Cox, M. C. Ellis, C. J. Atfield and A. C. Ferris, *J. Mol. Struct.*, 1994, **320**, 91.
- 15 T. H. Dunning, *J. Chem. Phys.*, 1971, **55**, 716.
- 16 Gaussian 92, M. J. Frisch, G. W. Trucks, M. Head-Gordon, P. M. W. Gill, M. W. Wong, J. B. Foresman, B. G. Johnson, H. B. Schlegel, M. A. Robb, E. S. Replogle, R. Gomperts, J. L. Andres, K. Raghavachari, J. S. Binkley, C. Gonzalez, R. L. Martin, D. J. Fox, D. J. Defrees, J. Baker, J. J. P. Stewart, S. Topiol and J. A. Pople, Gaussian Inc., Pittsburgh, PA, 1992; Gaussian 94 (Revision C. 2), M. J. Frisch, G. W. Trucks, H. B. Schlegel, P. M. W. Gill, B. G. Johnson, M. A. Robb, J. R. Cheesman, T. A. Keith, G. A. Petersson, J. A. Montgomery, K. Raghavachari, M. A. Al-Laham, V. G. Zakrzewski, J. V. Ortiz, J. B. Foresman, J. Cioslowski, B. B. Stefanov, A. Nanayakkara, M. Challacombe, C. Y. Peng, P. Y. Ayala, W. Chen, M. W. Wong, J. L. Andres, E. S. Replogle, R. Gomperts, R. L. Martin, D. J. Fox, J. S. Binkley, D. J. Defrees, J. Baker, J. P. Stewart, M. Head-Gordon, C. Gonzalez and J. A. Pople, Gaussian Inc., Pittsburgh, PA, 1995.
- 17 W. J. Hehre, L. Radom, P. v. R. Schleyer and J. A. Pople, *Ab Initio Molecular Orbital Theory*, John Wiley and Sons, New York, 1986.
- 18 R. French, L. Hedberg, K. Hedberg, G. L. Gard and B. M. Johnson, *Inorg. Chem.*, 1983, **22**, 892.
- 19 M. Torrent, P. Gili, M. Duran and M. Solà, *J. Chem. Phys.*, 1996, **104**, 9499.
- 20 A. J. H. Wachters, *J. Chem. Phys.*, 1970, **52**, 1033.
- 21 C. M. Huntley, G. S. Laurensen and D. W. H. Rankin, *J. Chem. Soc., Dalton Trans.*, 1980, 954.
- 22 S. Cradock, J. Koprowski and D. W. H. Rankin, *J. Mol. Struct.*, 1981, **77**, 113.
- 23 A. S. F. Boyd, G. S. Laurensen and D. W. H. Rankin, *J. Mol. Struct.*, 1981, **71**, 217.
- 24 A. W. Ross, M. Fink and R. Hildebrandt, in *International Tables for Crystallography*, Vol. C, ed. A. J. C. Wilson, Kluwer Academic Publishers, Dordrecht, 1992, p. 245.
- 25 L. Hedberg and I. M. Mills, *J. Mol. Spectrosc.*, 1993, **160**, 117.
- 26 F. Preuss, W. Towae and J. Woitschach, *Z. Naturforsch., Teil B*, 1980, **35**, 817.